

## Supporting Information

# W Exsolution Promotes the In-situ Reconstruction of NiW Electrode with Rich Active Sites for Electrocatalytic Oxidation of 5-hydroxymethylfurfural

Gang Xu<sup>a,b</sup>, Chenyu Chen<sup>a,b,c</sup>, Mengxia Li<sup>a,b,c</sup>, Xinyi Ren<sup>d</sup>, Lianggao Hu<sup>c</sup>, Chengrong Wu<sup>c</sup>, Yu Zhuang<sup>c</sup>,  
Fan Wang<sup>\*c</sup>

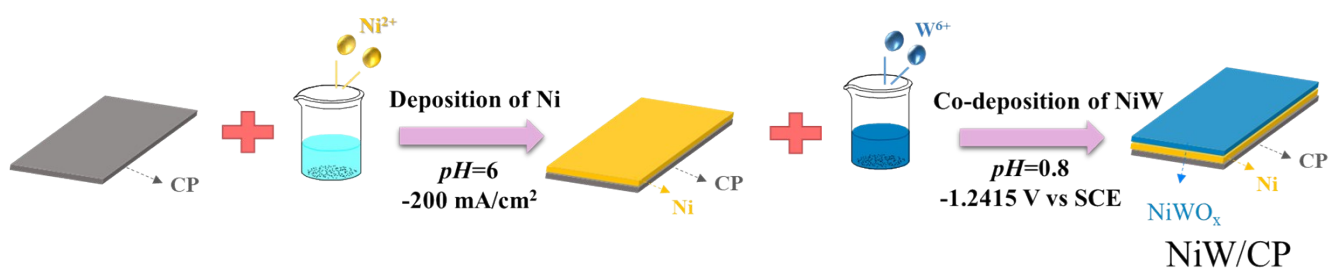
<sup>a</sup> Fujian Provincial Key Laboratory of Advanced Materials Oriented Chemical Engineering, College of Chemistry and Material Science, Fujian Normal University, Fuzhou 350007, China

<sup>b</sup> Fujian Provincial Key Laboratory of Polymer Materials, College of Chemistry and Materials Science, Fujian Normal University, Fuzhou 350007, China.

<sup>c</sup> Fujian Eco-materials Engineering Research Center, School of Ecological Environment and Urban Construction, Fujian University of Technology, Fuzhou 350118, China

<sup>d</sup> Dalian Institute of Chemical Physics, Chinese Academy of Sciences, 457 Zhongshan Road, Dalian 116023, China

\* Corresponding author: fanan\_wang@fjut.edu.cn (F.N. Wang)



**Scheme S1** The scheme of the fabrication procedures for NiW/CP.

**Notes:** The NiW/CP electrode was fabricated by a simple two-step electro-deposition. The first step was for the deposition of Ni base on the CP substrate (Ni-CP), and then the second was for the co-deposition of NiW layer on the Ni-CP substrate. This could be inferred from the ICP-MS results in **Table S1 and S2**. About  $18.6 \mu\text{g/mL}$  Ni was dissolved after the Ni/CP was immersed in the second-step electrolyte for 5 mins, while much fewer Ni ( $2.1 \mu\text{g/mL}$ ) was found in the electrolyte after 5-min cathodic deposition with W source. Moreover, the Ni in the samples from the electrolytes after the second electro-deposition without W source for Ni-2/CP ( $15.8 \mu\text{g/mL}$ ) was close to that after immersed, indicating that the Ni along cannot be deposited under the condition of second deposition without W. The amount of Ni ( $28.5 \text{ mg/mg}$ ) and W ( $1.8 \text{ mg/mg}$ ) on the NiW/CP was close to Ni ( $29.5 \text{ mg/mg}$ ) on Ni/CP and W ( $1.9 \text{ mg/mg}$ ) on the W/CP, respectively, confirming the co-deposition of NiW layer in the second deposition step.

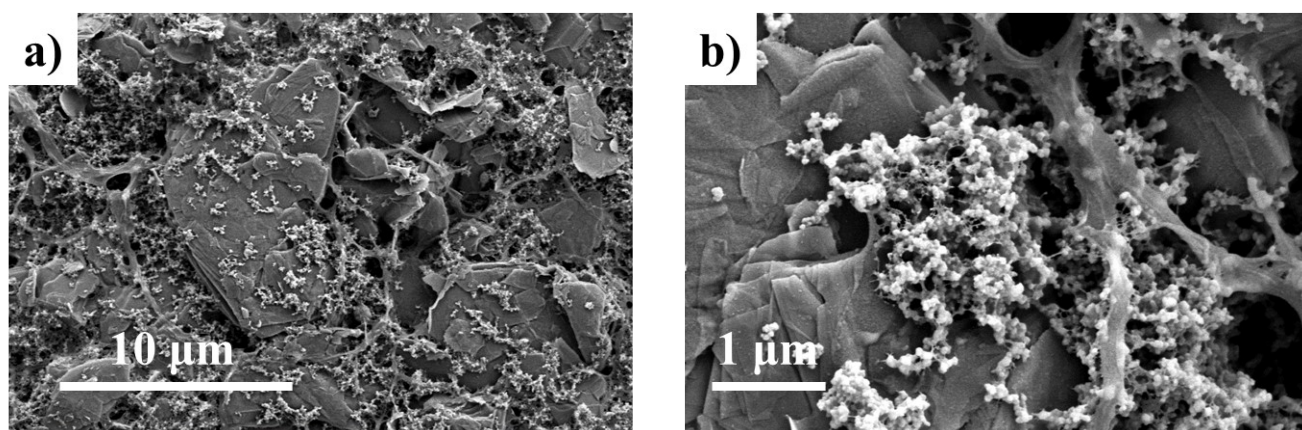


**Fig. S1** SEM images of CP.

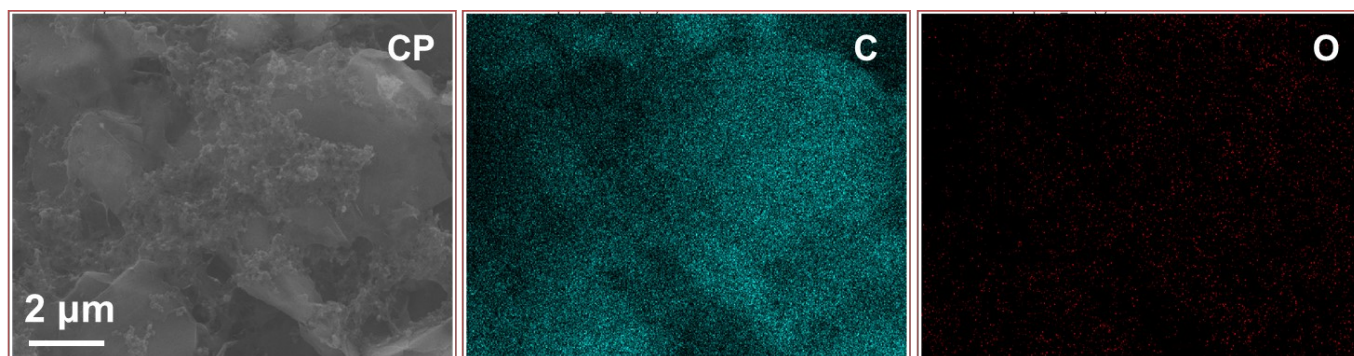


**Fig. S2** EDS-mapping images of CP.

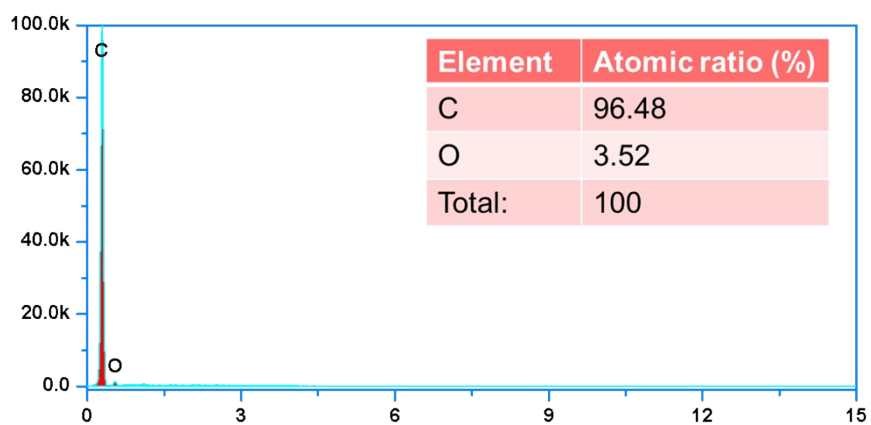


**Fig. S3** Element compositions of CP from SEM-EDS analysis. The only detected elements were C and O on the surface of CP.

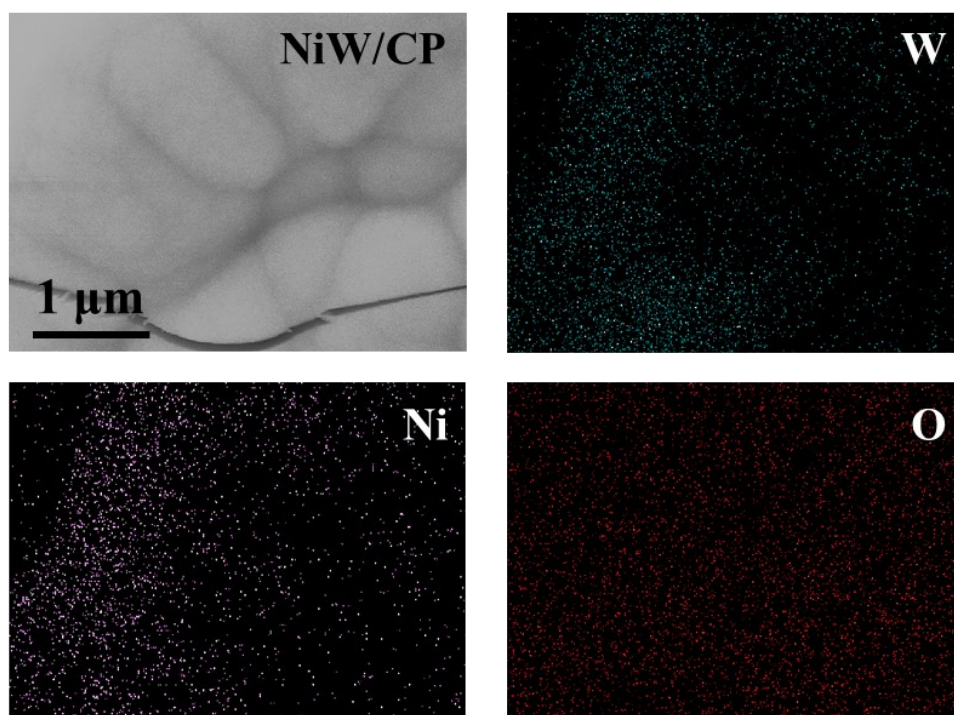


**Fig. S4** EDS-mapping images of NiW/CP.

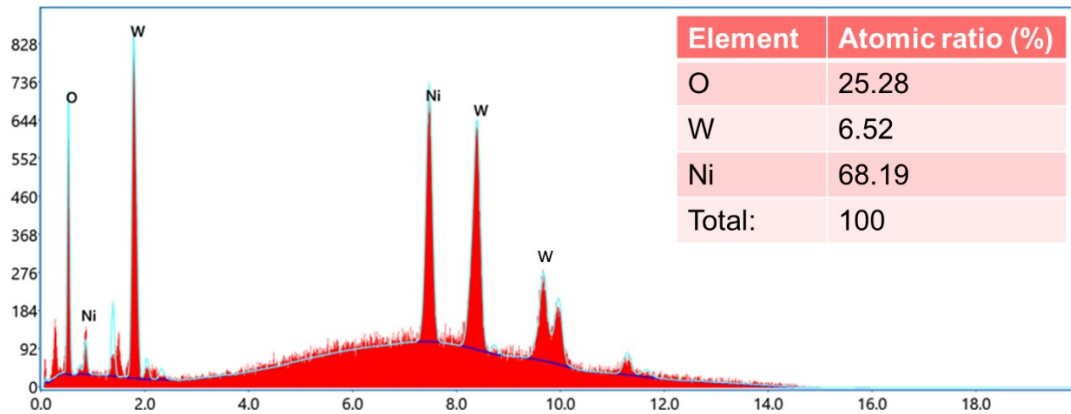


**Fig. S5** Element compositions of the NiW/CP from SEM-EDS analysis. The atomic ratio of Ni/W is 10.5.

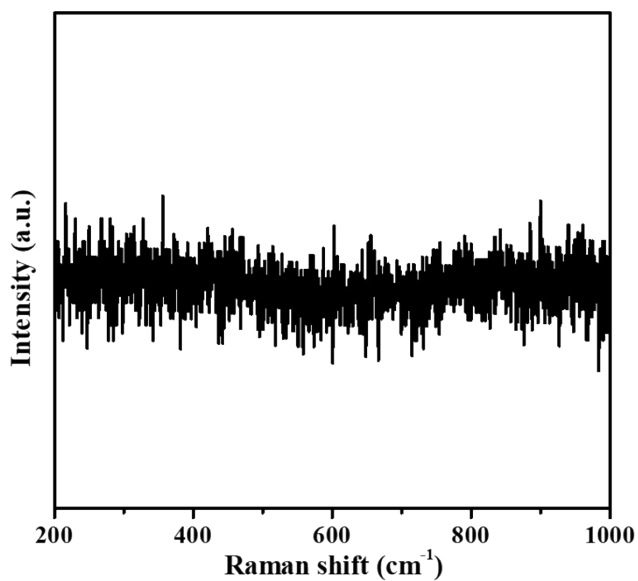


**Fig. S6** Raman spectrum of Ni/CP.

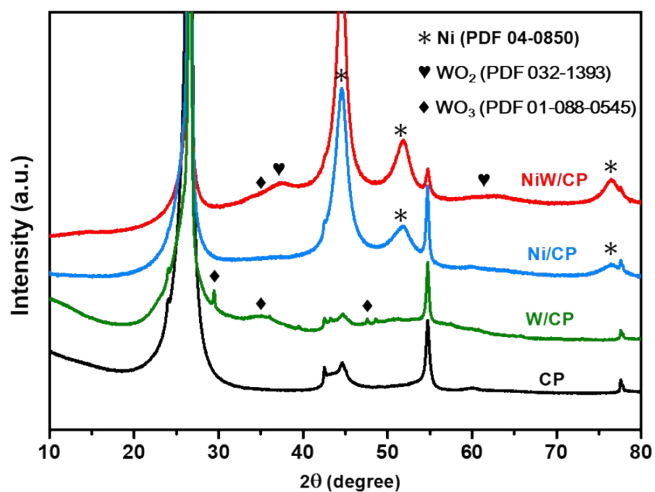


**Fig. S7** XRD spectra of NiW/CP, Ni/CP, W/CP and CP.

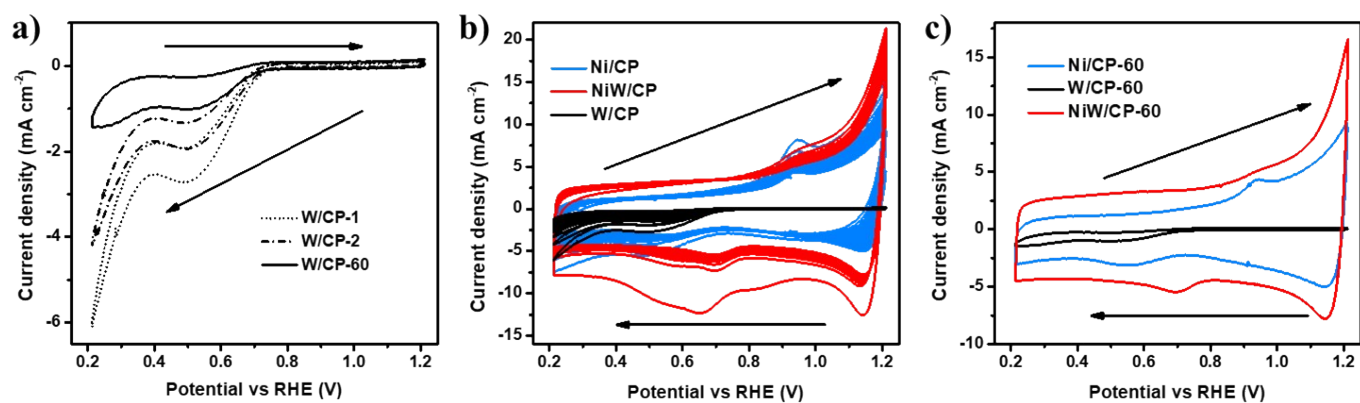


**Fig. S8** CV plots of different cycles for W/CP, Ni/CP and NiW/CP in 1 M KOH.

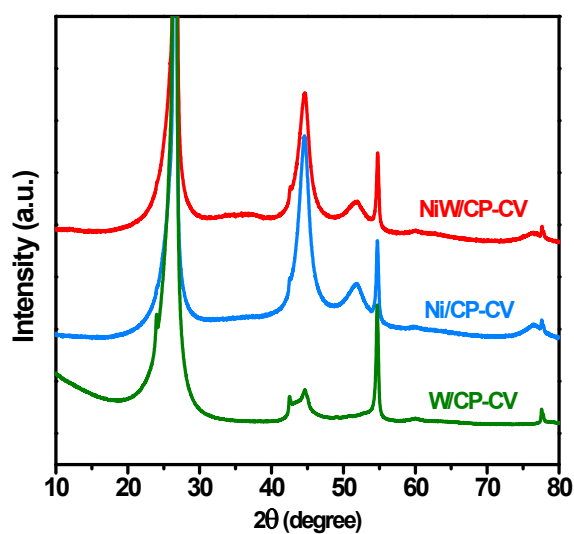


**Fig. S9** XRD spectra of NiW/CP, Ni/CP and W/CP after CV stabilization.

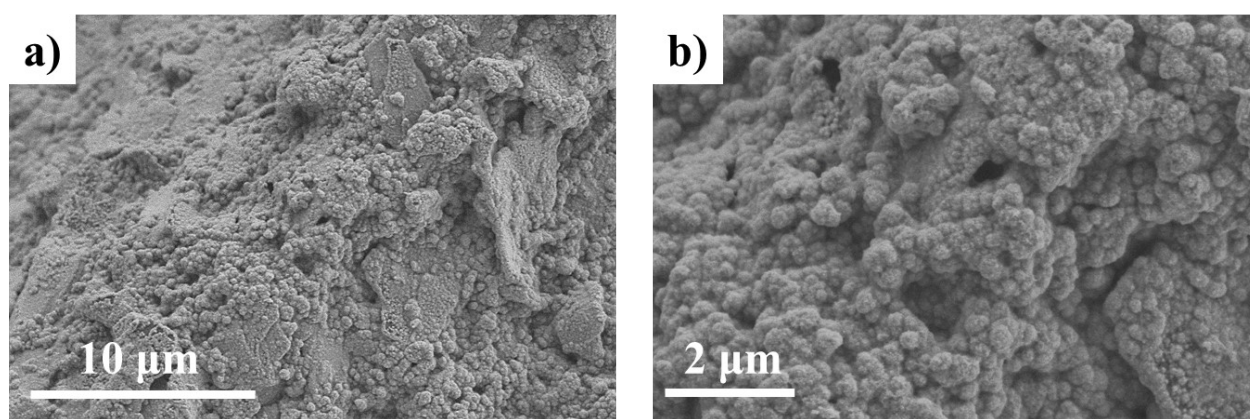


**Fig. S10** SEM images of Ni/CP after CV scan, with almost unchanged morphology by comparison to the as-prepared Ni/CP.

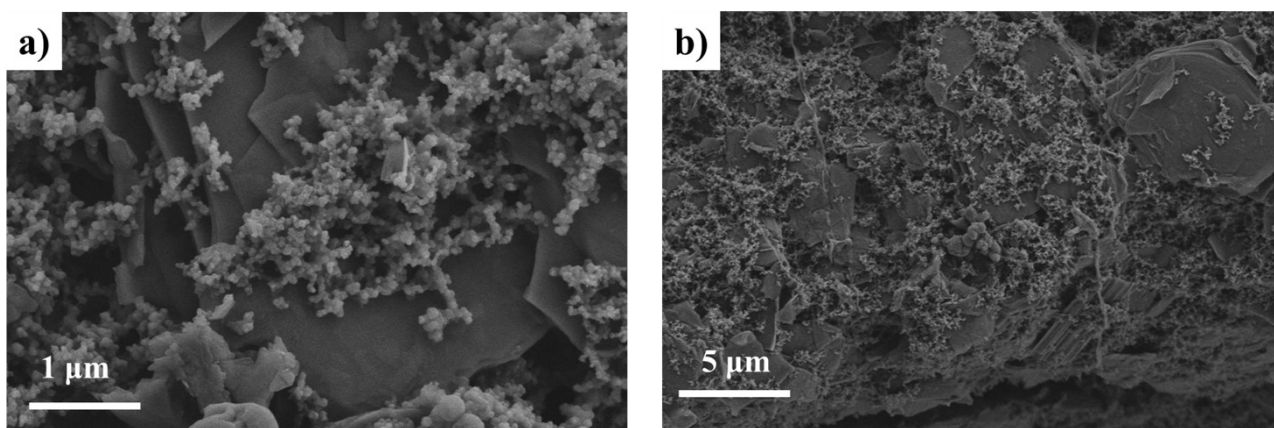


**Fig. S11** SEM images of W/CP after CV scan. The W layer was basically lost, with the morphology of CP substrate visible.

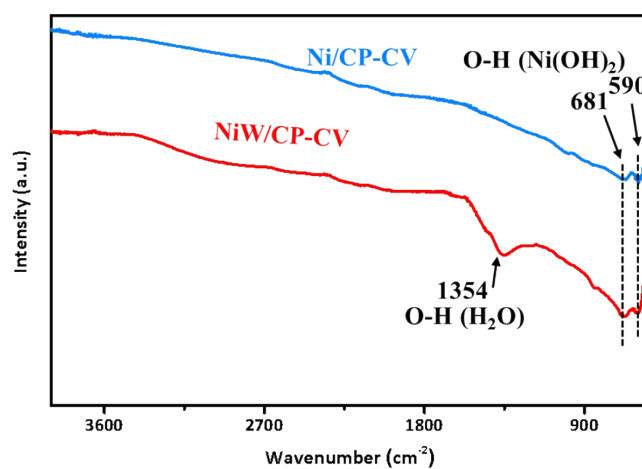


**Fig. S12** The ATR-FTIR spectra of Ni/CP and NiW/CP after CV stabilization.

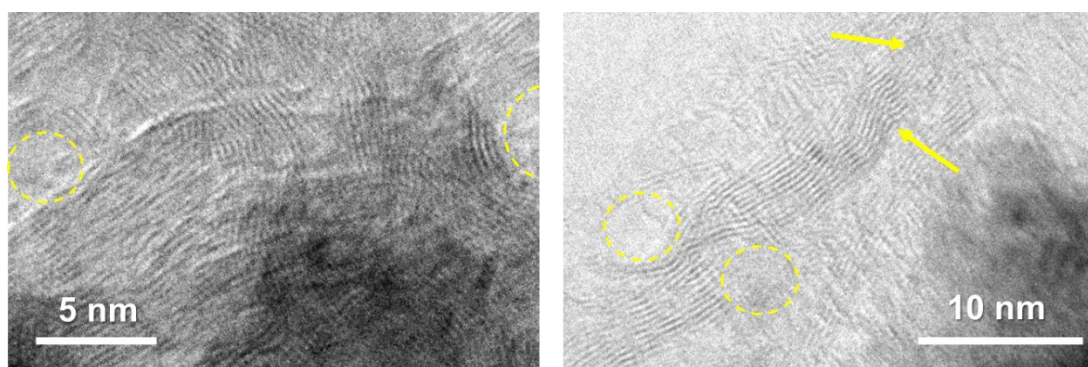


**Fig. S13** TEM images from different area of NiW/CP after CV stabilization

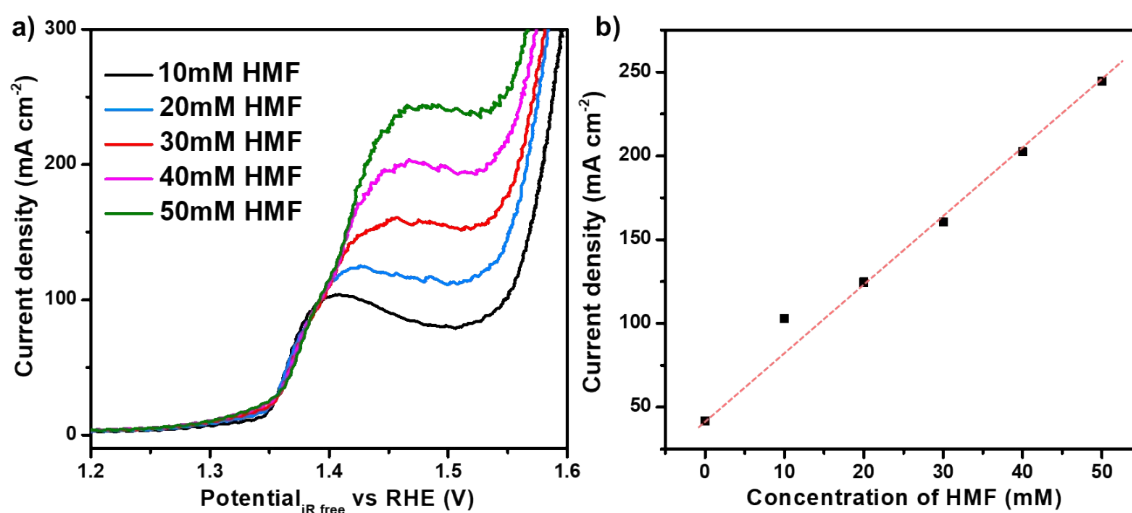


**Fig. S14** a) The LSVs of NiW/CP in 1 M KOH solution with different concentrations of HMF; b) the variation of the summit current density before 1.5 V with the concentration of HMF.

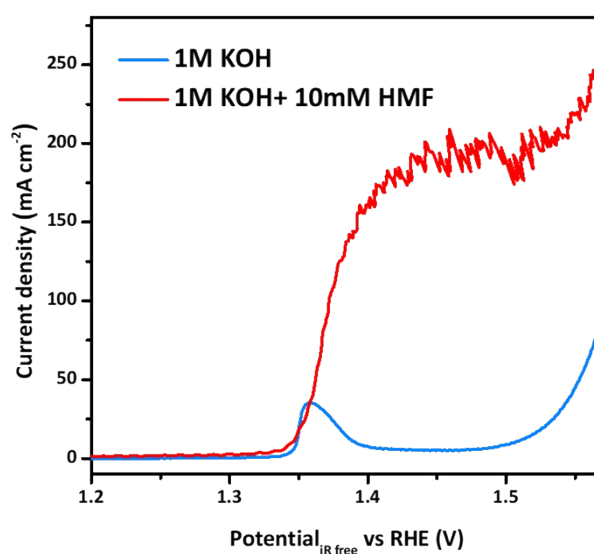


**Fig. S15** LSVs on NiW/NF in 1 M KOH solution with and without 10 mM HMF.

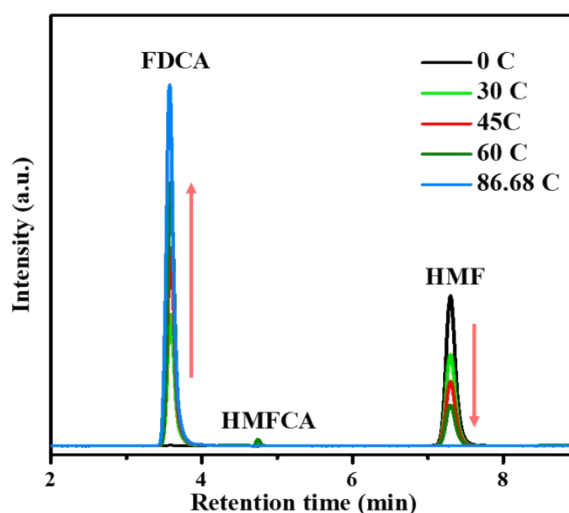


**Fig. S16** HPLC chromatogram over charges on NiW/CP in 1 M KOH with 5 mM HMF.

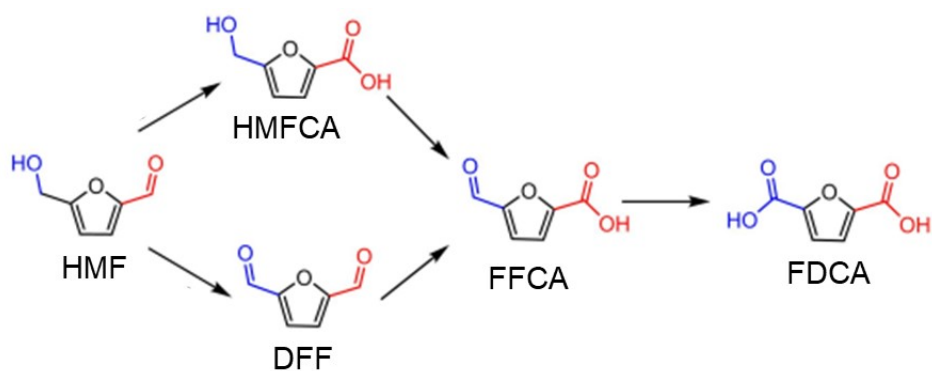


**Fig. S17** Reaction route for HMF to FDCA.

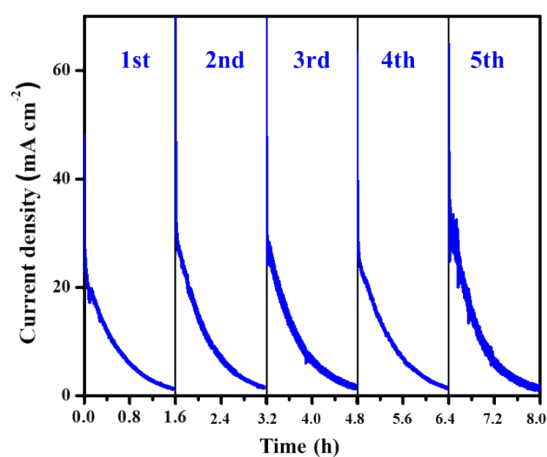


**Fig. S18** Current-time curves in 5 successive runs on NiW/CP in separated 30 mL 1 M KOH with 5 mM HMF.

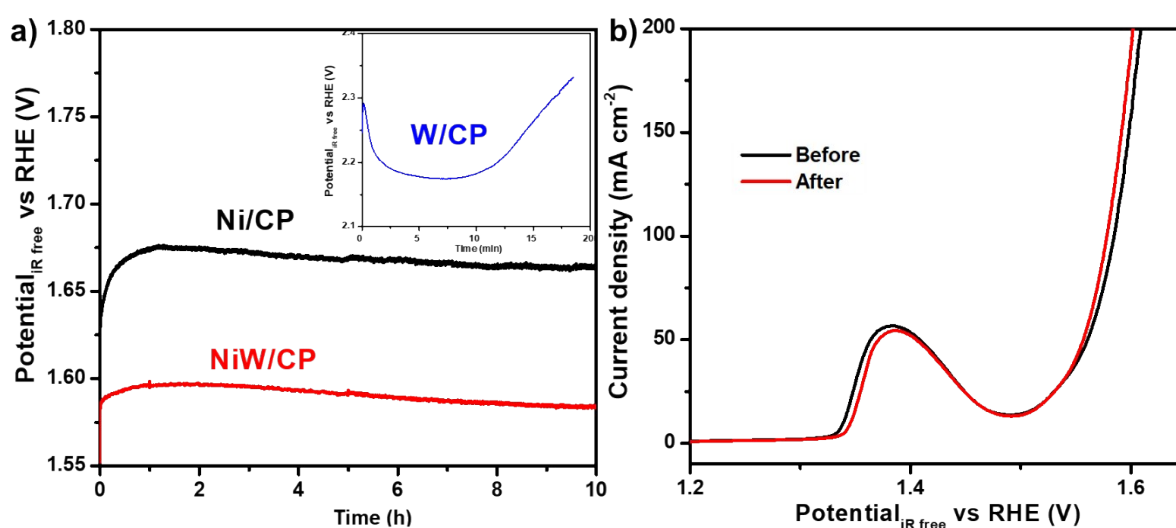


**Fig. S19** a) The long-time stability test for NiW/CP, Ni/CP and W/CP in 1 M KOH at a current density of 100 mA cm<sup>-2</sup>; b) the LSVs of NiW/CP in separated solutions of 1 M KOH before and after 10 h stability test.

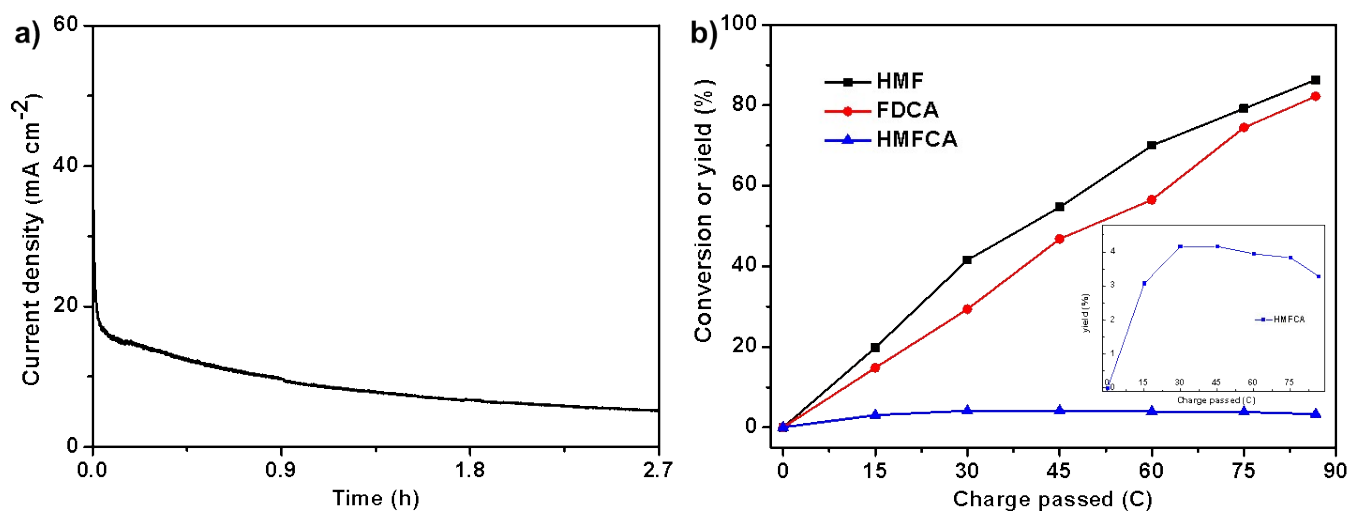


**Fig. S20** a) The current-time curve and b) the conversion of HMF or yield of FDCA and HMFCa on Ni/CP in 30 mL 1 M KOH with 5 mM HMF. It took over 2.7 h to pass 86.68 C charge on Ni/CP, with only 81% HMF conversion and 78% FDCA yield.

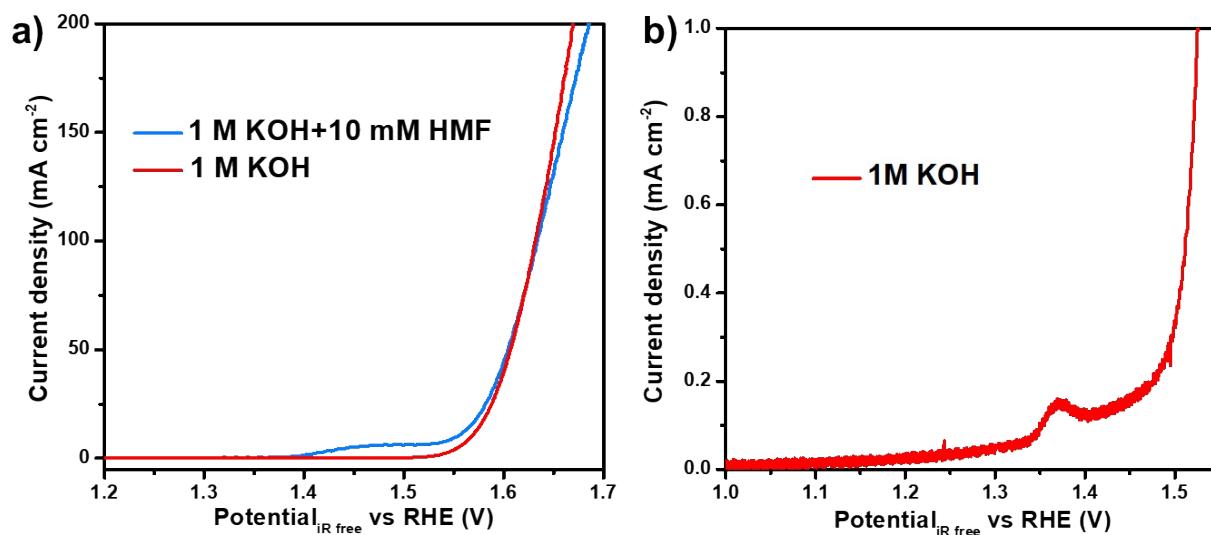


**Fig. S21** a) LSVs on Ni-2/CP in 1 M KOH solution with 10 mM HMF; b) the enlarged plot of a) from 1.0 V to 1.55 V.

**Notes:** The Ni-2/CP electrode was fabricated by the two electro-deposition steps but without W source. As discussed before, the Ni base after the first deposition was dissolved by the acidic solution in the second electrodeposition, and could be co-deposited back with the W source. While without the W source, the dissolved Ni ion could not be re-deposited, as indicated by the ICP results in Table S1 that the Ni in the solution after the second deposition of Ni-2/CP was far more than that of NiW/CP. The dramatic wastage of Ni on the Ni-2/CP was further supported by the much lower oxidation peak from the LSV in 1 M KOH solution in Fig. S17 b), and was ascribed to its much poorer activity.

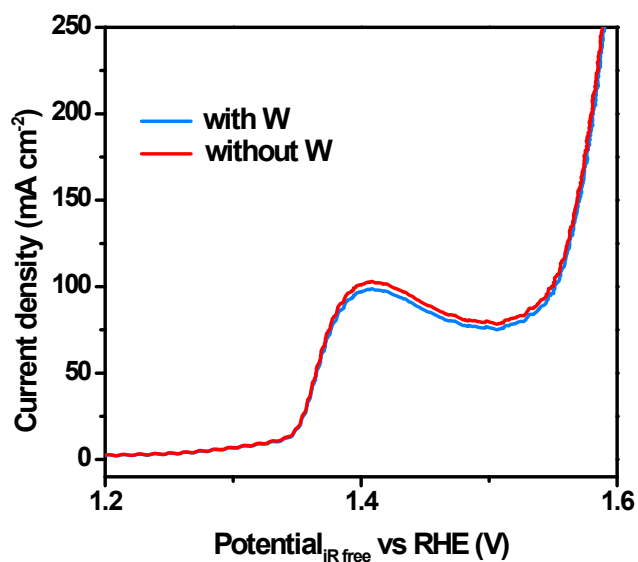


**Fig. S22** LSVs on NiW/CP in 1 M KOH solution with 10 mM HMF with or without W (17  $\mu\text{g}/\text{mL}$ ) dissolved.

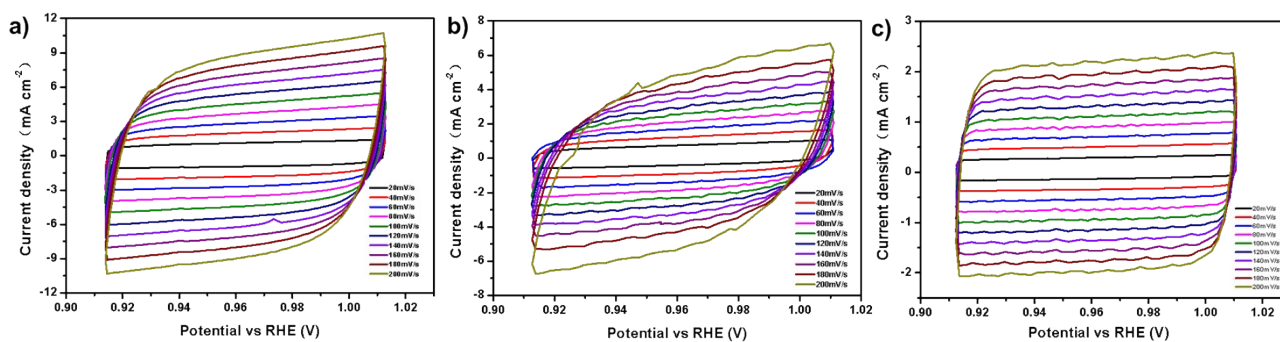


**Fig. S23** The CV between 0.91 and 1.01 V (vs RHE) at different scan rate from 20 to 200  $\text{mV}\cdot\text{s}^{-1}$  for a) NiW/CP, b) Ni/CP and c) W/CP

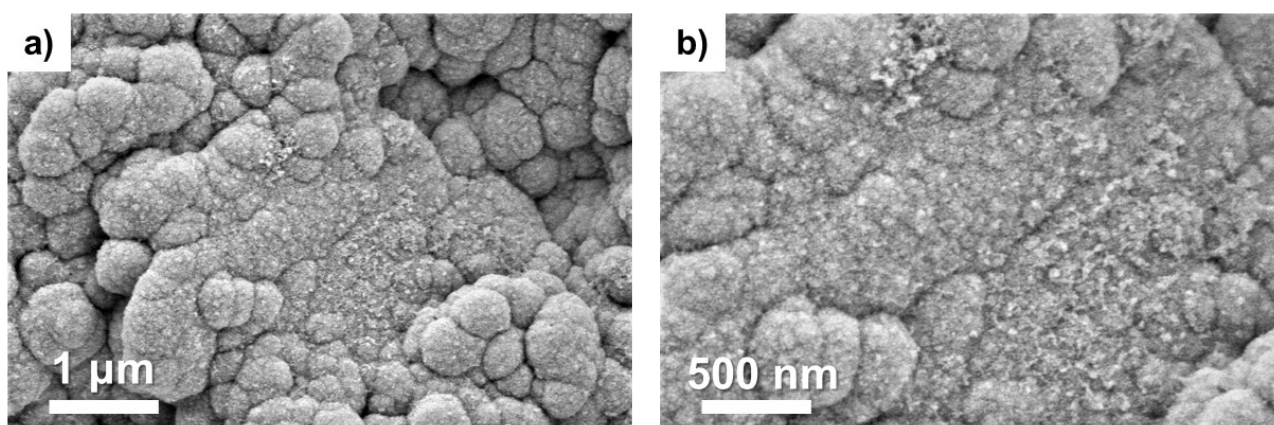


**Fig. S24** a, b) SEM images of NiW/CP after CV (before HMFOR).

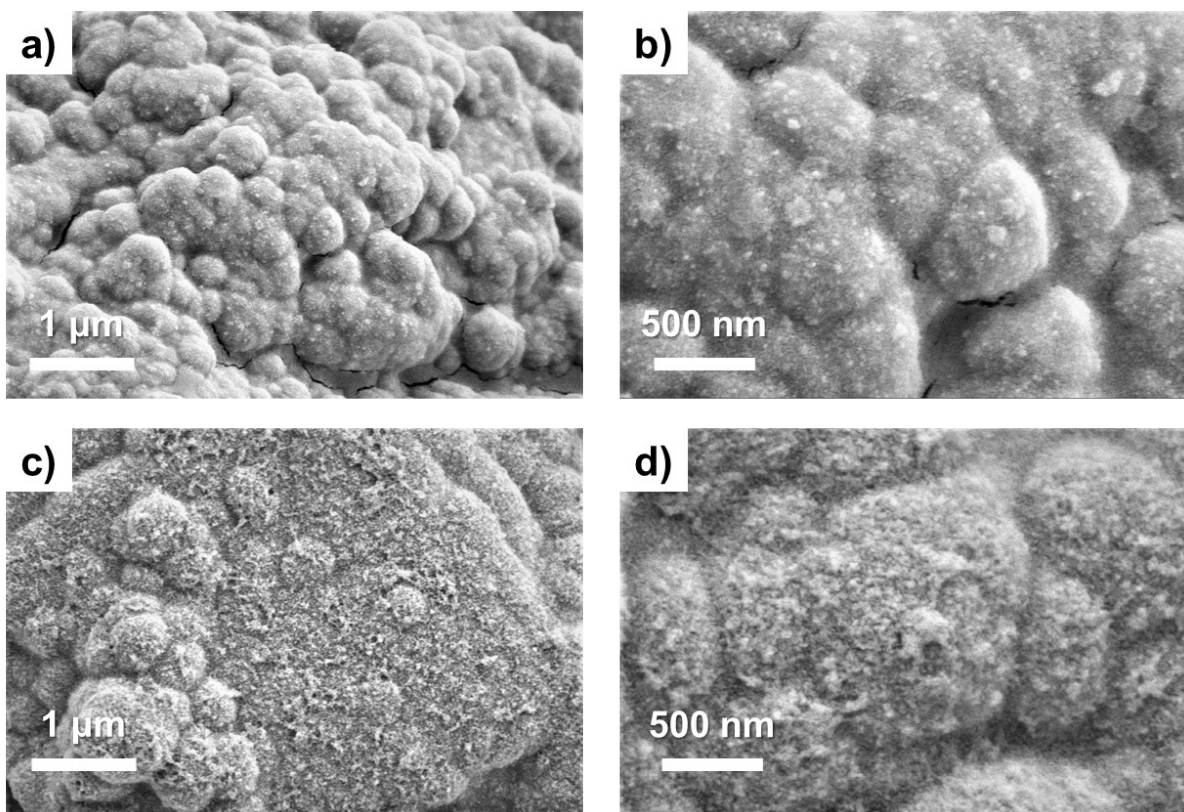


**Fig. S25** SEM images of Ni/CP a, b) after CV (before HMFOR) and c, d) after HMFOR.

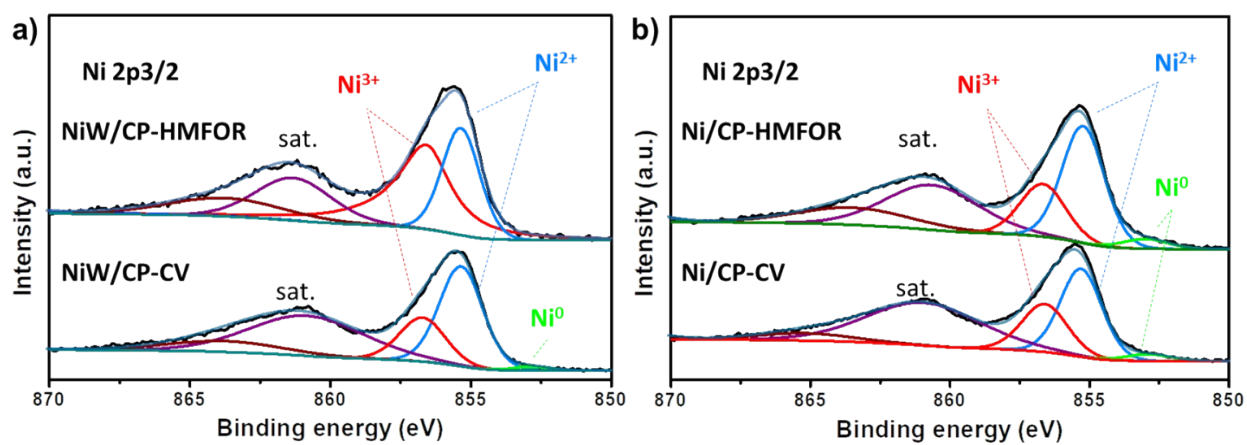


**Fig. S26** XPS spectra of Ni 2p<sub>3/2</sub> before and after HMFOR for a) NiW/CP and b) Ni/CP.

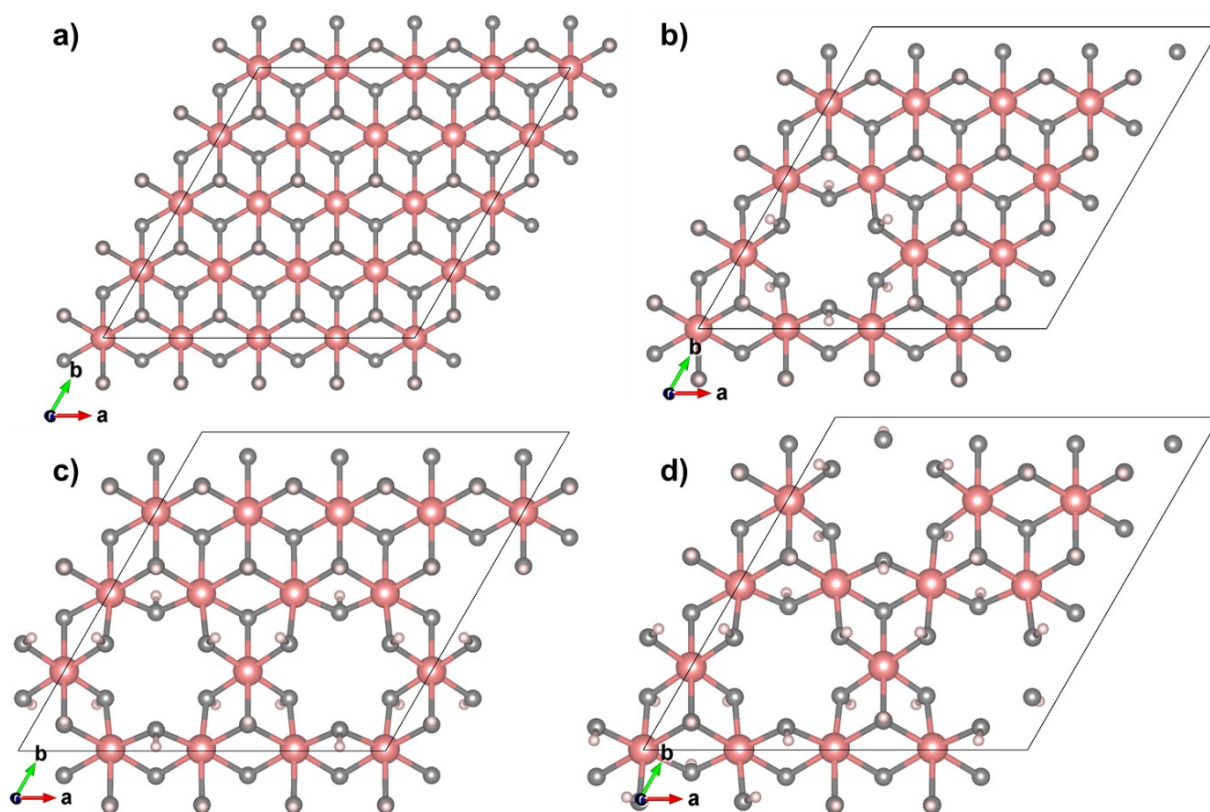
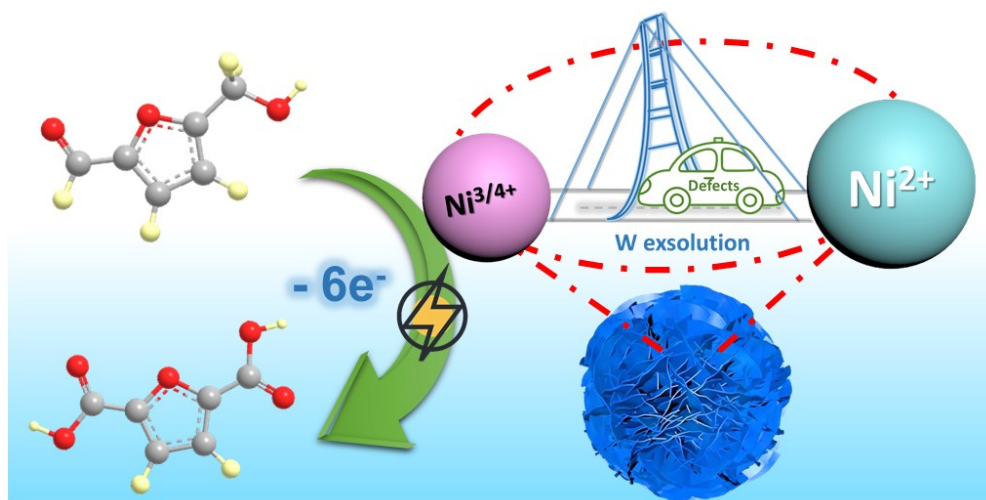


**Fig. S27** Top view of a) the pristine  $\text{Ni}(\text{OH})_2$ , and the  $\text{Ni}_{1-x}(\text{OH})_2$  with b) one Ni vacancy ( $x=0.0625$ ), c) two Ni vacancies ( $x=0.125$ ), d) three Ni vacancies ( $x=0.1875$ ). The Ni, O, H atoms were represented with dark pink, grey and light pink balls, respectively.



**Scheme S2** The promotion of W exsolution from the NiW layer on the formation of high-valence Ni sites with superior activity towards HMFOR.

**Table S1** The concentrations of Ni or W collected from different electrolytes by ICP-MS. Specifically, NiW/CP-de or Ni-2/CP-de represented the samples from the electrolytes after the second electro-deposition with or without W source for NiW/CP or Ni-2/CP, respectively. Ni/CP-im represented the sample from the electrolytes of second electro-deposition with Ni/CP immersed for 5 min. The NiW/CP, Ni/CP and W/CP under columns of CV-x (x=1, 2, 10 and 60) represented the samples from the 1 M KOH electrolyte after x cycles of CV on the NiW/CP, Ni/CP and W/CP, respectively.

	Ni ( $\mu\text{g/mL}$ )				W ( $\mu\text{g/mL}$ )			
	CV-1	CV-2	CV-10	CV-60	CV-1	CV-2	CV-10	CV-60
NiW/CP-de	2.13 $\pm$ 0.05				4.53 $\pm$ 0.01			
Ni/CP-im	18.57 $\pm$ 0.04				4.57 $\pm$ 0.03			
Ni-2/CP-de	15.76 $\pm$ 0.05				-			
NiW/CP	0.03 $\pm$ 0.01	0.07 $\pm$ 0.01	0.17 $\pm$ 0.02	0.37 $\pm$ 0.03	10.71 $\pm$ 0.05	14.53 $\pm$ 0.06	16.74 $\pm$ 0.05	17.18 $\pm$ 0.04
Ni/CP	0.05 $\pm$ 0.01	0.08 $\pm$ 0.01	0.25 $\pm$ 0.03	0.53 $\pm$ 0.03	-	-	-	-
W/CP	-	-	-	-	15.63 $\pm$ 0.06	17.72 $\pm$ 0.03	18.91 $\pm$ 0.05	19.07 $\pm$ 0.04

**Table S2** The weight percentage of Ni or W collected in one piece of modified CP for NiW/CP, Ni/CP and W/CP by ICP-MS. The columns of fresh, CV-60 and HMFOR-5 cycles represented the samples as-prepared, after 60 cycles of CV and after 5 successive runs of HMFOR, respectively. Each data was repeated for 3 times with 3 different pieces of modified CP.

	Ni (wt. %)			W (wt. %)		
	fresh	CV-60	HMFOR-5 cycles	fresh	CV-60	HMFOR-5 cycles
NiW/CP	28.51 $\pm$ 0.03	28.43 $\pm$ 0.05	28.12 $\pm$ 0.02	1.82 $\pm$ 0.05	under detection	under detection
Ni/CP	29.47 $\pm$ 0.05	28.79 $\pm$ 0.05	28.85 $\pm$ 0.06	-	-	-
W/CP	-	-	-	1.94 $\pm$ 0.05	under detection	under detection

**Table S3** The comparisons of electro-chemical performance among this work and reported electrode. All the performance were tested in 1 M KOH at 25 °C, with 10 mM HMF for LSV, unless otherwise noted.

Catalyst	Electrode substrate	LSV performance potentail ( $V_{RHE}$ ) / current density ( $\text{mA cm}^{-2}$ )	Chronoamperometry performance					
			Total charge (C)	Reaction potential ( $V_{RHE}$ )	Reaction time (min)	FE (%)	FDCA yield (%)	Cycl e
This work NiW	CP	1.27 / onset 1.36 / 10 1.38 / 80	86.68	1.38	96	95.5	95.6	5
	NF	1.38 / 150	-					
Ni nanosheet <sup>1</sup>	CP	1.33 / onset <sup>a</sup> 1.4 / 10 <sup>a</sup>	43.3	1.36	60	~95	99.4	3
Ni <sub>x</sub> B <sup>2</sup>	NF	1.40 / onset 1.45 / 100	58.2	1.45	30	~100	98.5	-
NiSe@NiO <sub>x</sub> <sup>3</sup>	NF	1.35 / onset 1.36 / 240	58	1.423	-	99	~100	6
Ni <sub>3</sub> N@C <sup>4</sup>	NF	1.38 / 50	174	1.45	-	99.0	98	6
S-Ni@C <sup>5</sup>	Carbon Cloth	1.35 / onset 1.47 / 40	86.84	1.473	270	96	96	5
NiCoBDC <sup>6,b</sup>	NF	1.54 / 10	-	1.55	240	78.8	99	4
NiFe LDH <sup>7</sup>	CP	1.25 / onset 1.32 / 20	57.79	1.33	90	98.6	98	4
NiCoFe LDH <sup>8,c,d</sup>	CP	1.51 / 20	-	1.52	60	-	81.6	-
CoO-CoSe <sub>2</sub> <sup>9</sup>	NF	1.3 / onset 1.4 / 50 <sup>a</sup>	86.68	1.43	57	97.9	99	5
CoNW <sup>10</sup>	NF	1.311 / 10 1.764 / 100	289.5	1.469	-	96.6	98	5
NiCoMn LDH <sup>11,c,e</sup>	NF	1.42 / onset 1.58 / 50	20.3	1.5	150	65	91.7	4

<b>Cu<sub>x</sub>S@NiCo LDH</b>	Cu foam	1.3 / 87 1.35 / 180.6	57.6	1.32	~75	99	99	5
<b>t-NiCo-MOF<sup>12,f</sup></b>	NF	1.4 / 600~730	57.8	-	~66	98	~100	5

<sup>a</sup> The data were evaluated from the corresponding LSV curves.

<sup>b</sup> Basic solution was 0.1 M KOH.

<sup>c</sup> Basic solution was 1 M NaOH.

<sup>d</sup> The chronoamperometry test was conducted at 65 °C.

<sup>e</sup> The chronoamperometry test was conducted at 35 °C.

<sup>f</sup> The HMF concentration was 50 mM for LSV test.

**Table S4** Detailed deconvolution data of the Ni 2p<sub>3/2</sub> for Ni/CP and NiW/CP before and after HMFOR from XPS.

	Binding energy (eV)	Atomic content (%)			
		Ni/CP	NiW/CP	Ni/CP-HMFOR	NiW/CP-HMFOR
Ni <sup>0</sup>	852.9 ± 0.1	4.9	2.2	5.6	0
Ni <sup>2+</sup>	855.3 ± 0.1	59.4	61.3	63.5	39.6
Ni <sup>3+</sup>	856.6 ± 0.1	35.7	36.5	30.9	60.4

**Table S5** The total energy ( $E_{\text{tot}}$ ) of NiOOH, H<sub>2</sub>O, H<sub>2</sub>, and Ni<sub>1-x</sub>(OH)<sub>2</sub> (x=0, 0.0625, 0.1250, 0.1875) and the formation energy ( $E_f$ ) from Ni<sub>1-x</sub>(OH)<sub>2</sub> to NiOOH from the DFT calculations.

Item	$E_{\text{tot}}$ (eV)	$E_{\text{tot}}$ (eV)/unit	$E_f$ (eV)
NiOOH	-343.381	-21.4613	
H <sub>2</sub> O	-14.225		
H <sub>2</sub>	-6.758		
Ni <sub>1-x</sub> (OH) <sub>2</sub> , x=0.0000	-423.424	-26.4640	2.45
Ni <sub>1-x</sub> (OH) <sub>2</sub> , x =0.0625	-415.737	-25.9836	1.05
Ni <sub>1-x</sub> (OH) <sub>2</sub> , x =0.1250	-408.529	-25.5331	-0.31
Ni <sub>1-x</sub> (OH) <sub>2</sub> , x =0.1875	-401.426	-25.0891	-1.67

## Reference

1. X. Lu, K. H. Wu, B. Zhang, J. Chen, F. Li, B. J. Su, P. Yan, J. M. Chen and W. Qi, *Angew. Chem. Int. Ed. Engl.*, 2021, **60**, 14528-14535.
2. S. Barwe, J. Weidner, S. Cychy, D. M. Morales, S. Dieckhofer, D. Hiltrop, J. Masa, M. Muhler and W. Schuhmann, *Angew. Chem. Int. Ed. Engl.*, 2018, **57**, 11460-11464.
3. L. Gao, Z. Liu, J. Ma, L. Zhong, Z. Song, J. Xu, S. Gan, D. Han and L. Niu, *Appl. Catal. B-Environ.*, 2020, **261**.
4. N. Zhang, Y. Zou, L. Tao, W. Chen, L. Zhou, Z. Liu, B. Zhou, G. Huang, H. Lin and S. Wang, *Angew. Chem. Int. Ed. Engl.*, 2019, **58**, 15895-15903.
5. F. Kong and M. Wang, *ACS Appl. Energ. Mater.*, 2021, **4**, 1182-1188.
6. M. Cai, Y. Zhang, Y. Zhao, Q. Liu, Y. Li and G. Li, *J. Mater. Chem. A*, 2020, **8**, 20386-20392.
7. W.-J. Liu, L. Dang, Z. Xu, H.-Q. Yu, S. Jin and G. W. Huber, *ACS Catal.*, 2018, **8**, 5533-5541.
8. M. Zhang, Y. Liu, B. Liu, Z. Chen, H. Xu and K. Yan, *ACS Catal.*, 2020, **10**, 5179-5189.
9. X. Huang, J. L. Song, M. L. Hua, Z. B. Xie, S. S. Liu, T. B. Wu, G. Y. Yang and B. X. Han, *Green Chem.*, 2020, **22**, 843-849.
10. Z. Zhou, C. Chen, M. Gao, B. Xia and J. Zhang, *Green Chem.*, 2019, **21**, 6699-6706.
11. B. Liu, S. Xu, M. Zhang, X. Li, D. Decarolis, Y. Liu, Y. Wang, E. K. Gibson, C. R. A. Catlow and K. Yan, *Green Chem.*, 2021, **23**, 4034-4043.
12. X. Deng, M. Li, Y. Fan, L. Wang, X.-Z. Fu and J.-L. Luo, *Appl. Catal. B-Environ.*, 2020, **278**, 119339-119353.